Supporting Information

Novel Tetrazole Pt^{II} and Pd^{II} Complexes with Enhanced Water Solubility: Synthesis, Structural Characterization and Evaluation of Antiproliferative Activity

Tatiyana V. Serebryanskaya,[1] Alexander S. Lyakhov, [1] Ludmila S. Ivashkevich,[1] Yuri V. Grigoriev,[1] Andreii S. Kritchenkov,[2] Victor N. Khrustalev,[2,4] Alexander G. Tskhovrebov,*[2,3] Oleg A. Ivashkevich[1]

1 Research Institute for Physical Chemical problems, Belarusian State University, 14 Leningradskaya str., 220006 Minsk, Belarus; serebryanskaya.t@gmail.com

2 N.N. Semenov Federal Research Center for Chemical Physics, Russian Academy of Sciences, Ul. Kosygina 4, Moscow, Russian Federation; alexander.tskhovrebov@chph.ras.ru

3 Peoples' Friendship University of Russia, 6 Miklukho-Maklaya Street, Moscow, 117198, Russian Federation; vnkhrustalev@gmail.com

4 N.D. Zelinsky Institute of Organic Chemistry, Russian Academy of Sciences, 47 Leninsky Prosp., Moscow, Russian Federation

* Correspondence: alexander.tskhovrebov@chph.ras.ru

NMR spectroscopy

Table S1 ^{1}H and ^{13}C NMR spectra [δ and Δδ[a] (in parentheses), ppm, DMSO-d^6] of platinum(II) complexes.

L, geometry	^{1}H				^{13}C		
	C5–H	OH	α-CH_2	β-CH_2	C5	α-C	β-C
het, *cis*	10.20 (0.84)	5.20 (0.14)	4.62 (–0.20)	3.82 (–0.32)	145.30 (1.16)	52.15 (1.86)	58.40 (–0.60)
het, *trans*	10.14 (0.78)	5.21 (0.15)	4.63 (t) (–0.19)	3.84 (t) (–0.30)	145.49 (1.35)	52.14 (1.85)	58.44 (–0.56)
thm, *trans*	10.06 (0.72)	5.29 (0.95)	–	3.90 (0.03)	144.63 (1.31)	72.27 (2.53)	59.64 (–0.46)

[a] $\Delta\delta = \delta_{complex} - \delta_{ligand}$

IR spectroscopy

Table S2 IR bands (cm^{-1}) of het and its platinum(II) and palladium(II) complexes.

het	*trans*-$Pd(het)_2Cl_2$	*trans*-$Pt(het)_2Cl_2$	*cis*-$[Pt(het)_2Cl_2]$	Assignment
3373 vs br	3465 vs br	3547 vs	3442 vs 3368 s	ν(OH)
3144 vs	3147 s	3103 vs	3145 cp 3109 s	$\nu(CH)_{cycle}$
3009 s 2959 s 2922 vs 2858 s	3010 m 2968 m 2945 m 2885 m	3012 s 2942 s 2885 s	3017 m 2998 m 2959 m 2934 m 2880 m	$\nu(CH)_{cycle}$
1488 vs	1504 s	1513 s	1508 s	ν(C=N)
1435 s	1445 s	1460 s 1432 m	1447 s 1430 m	$\nu(N{=}N)_{cycle}$ $+ \delta(CH)_{as}$
1362 m 1332 s	1385 s 1354 s	1397 w 1362 m	1357 m 1343 m	$\delta(CH)_s$ + δ(OH)
1291 m	1304 s 1278 m	1319 s 1291 sh	1292 s	$\nu(N{-}N)_{cycle}$
1245 m 1158 s	1251 s 1176 s 1151 s	1247 m 1183 vs	1233 m 1183 s 1152 w	ν_{cycle} $+ \rho(CH)_{alkyl}$ + ρ(OH)
1076 s 1055 s 1026 s 979 vs 897 vs	1091 m 1051 vs 885 w	1099 s 1064 s 1046 s 1026 s 947 w 903 m	1107 s 1094 vs 1060 vs 1013 m 946 w 889 w	ν,δ_{cycle} $+ \nu(C{-}O)$ $+ \rho(CH)_{cycle}$
876 s	868 m	870 m	866 m	$\gamma(CH)_{cycle}$
733 vs 681 vs br	662 s	680 m 657 s	751 w br 674 m 645 m	γ_{cycle}
502 vs	525 w	506 s	560 w br 500 w	ω(OH)
	470 s	407 m		$\nu(Pt{-}N) + \delta_{cycle}$
	356 s	352 s	345 s	ν(Pt–Cl)

Table S3 IR bands (cm^{-1}) of thm and its platinum(II) and palladium(II) complexes.

thm	*trans*-$Pd(thm)_2Cl_2$	*trans*-$[Pt(thm)_2Cl_2]$	Assignment
3373 vs br	3454 s 3300 s	3463 s 3315 c	ν(OH)
3120 vs	3088 s	3089 s	$\nu(CH)_{cycle}$
3009 s 2959 s 2922 vs 2858 s	2973 m 2910 w 2890 w	2977 s 2910 m 2891 w	$\nu(CH)_{alkyl}$
1629 s 1550 m	1626 w br	1624 w br	δ(OH)
1461 s	1499 m 1465 m	1501 s 1466 s	$\nu(C{=}N) + \delta(CH)_{as}$
1408 s	1423 m	1425 s	$\nu(N{=}N)_{cycle}$ δ(OH)
	1379 s	1380 s	$\delta(CH)_s$
1293 s 1245 m	1301 m 1279 m 1248 w	1303 m 1281 m	$\nu(N–N)_{cycle}$
1204 m 1127 m	1210 w 1189 s 1148 m	1220 m 1189 s 1150 m	ν_{cycle} $+ \rho(CH)_{alkyl}$ $+\rho(OH)$
1085 w 1032 vs 1008 s	1112 m 1089 s 1043 s 1009 vs	1112 m 1092 s 1045 s 1007 vs	ν,δ_{cycle} $+ \nu(C–O)$ $+ \rho(CH)_{cycle}$
909 s	894 m	892 s	$\gamma(CH)_{cycle}$
	875 w	838 w	δ_{cycle}
721 m 652 vs	665 vs	667 s	γ_{cycle}
590 vs 509 vs	617 m 553 m br	617 m 557 m br	ω(OH)
482 s 433 s	456 m	460 br	
	408 s	408 s	$\nu(Pt–N) + \delta_{cycle}$
	348 m	343 m	ν(Pt–Cl)

TGA analysis

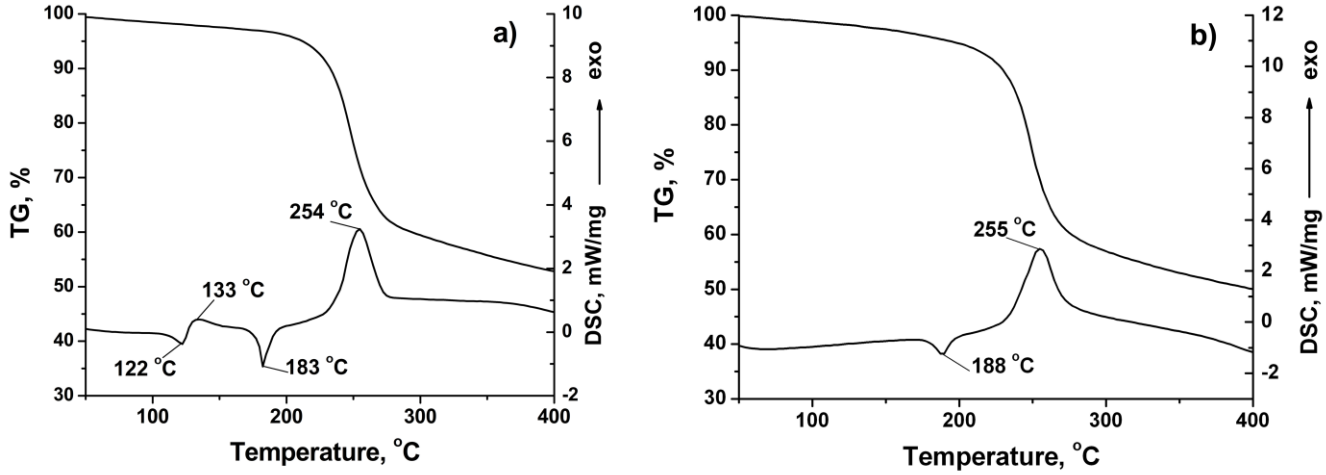

Figure S1. TG and DSC curves of (*a*) *cis*-[Pt(het)$_2$Cl$_2$] and (*b*) *trans*-[Pt(het)$_2$Cl$_2$].

HPLC data

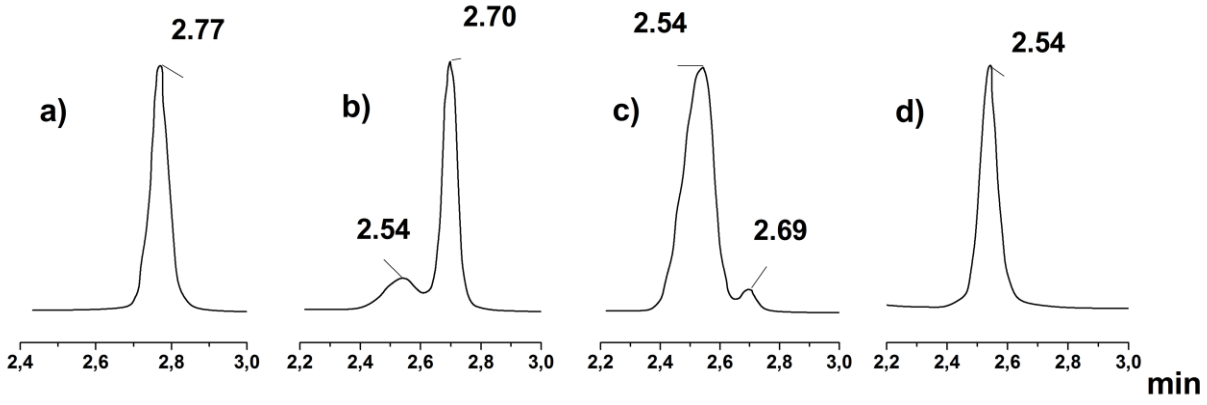

Figure S2. HPLC chromatograms for (*a*) *cis*-[Pt(het)$_2$Cl$_2$]; (*b*) *cis*-[Pt(het)$_2$Cl$_2$] after heating up to 110 ºC; (*c*) *cis*-[Pt(het)$_2$Cl$_2$] after heating up to 150 ºC; (*d*) *trans*-[Pt(het)$_2$Cl$_2$].

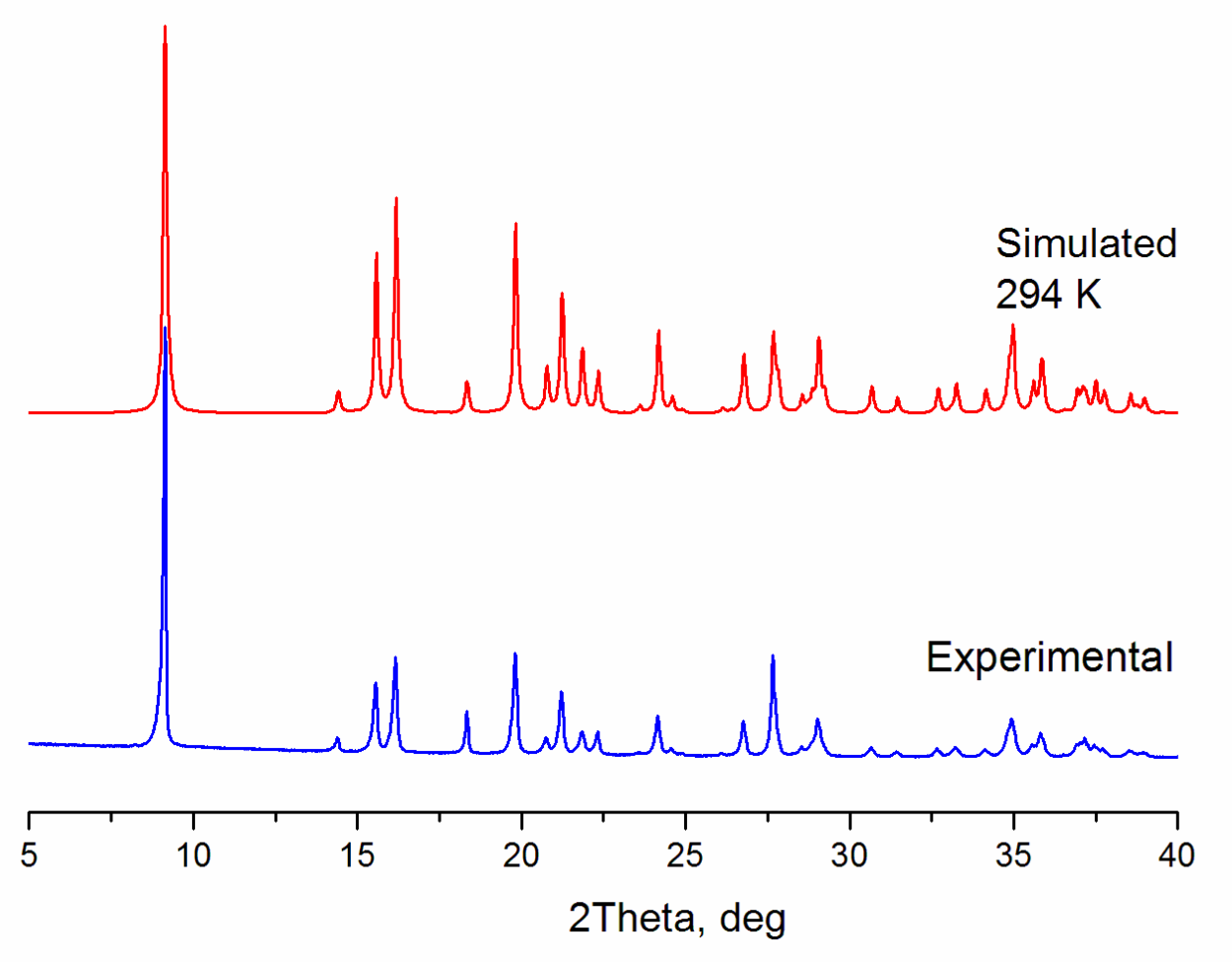

Figure S3. Simulated (top) and experimental (bottom) powder XRD patterns of *trans*-[Pt(het)$_2$Cl$_2$] (complex **4**) (CuKα radiation). The simulated pattern was calculated using PLATON program.

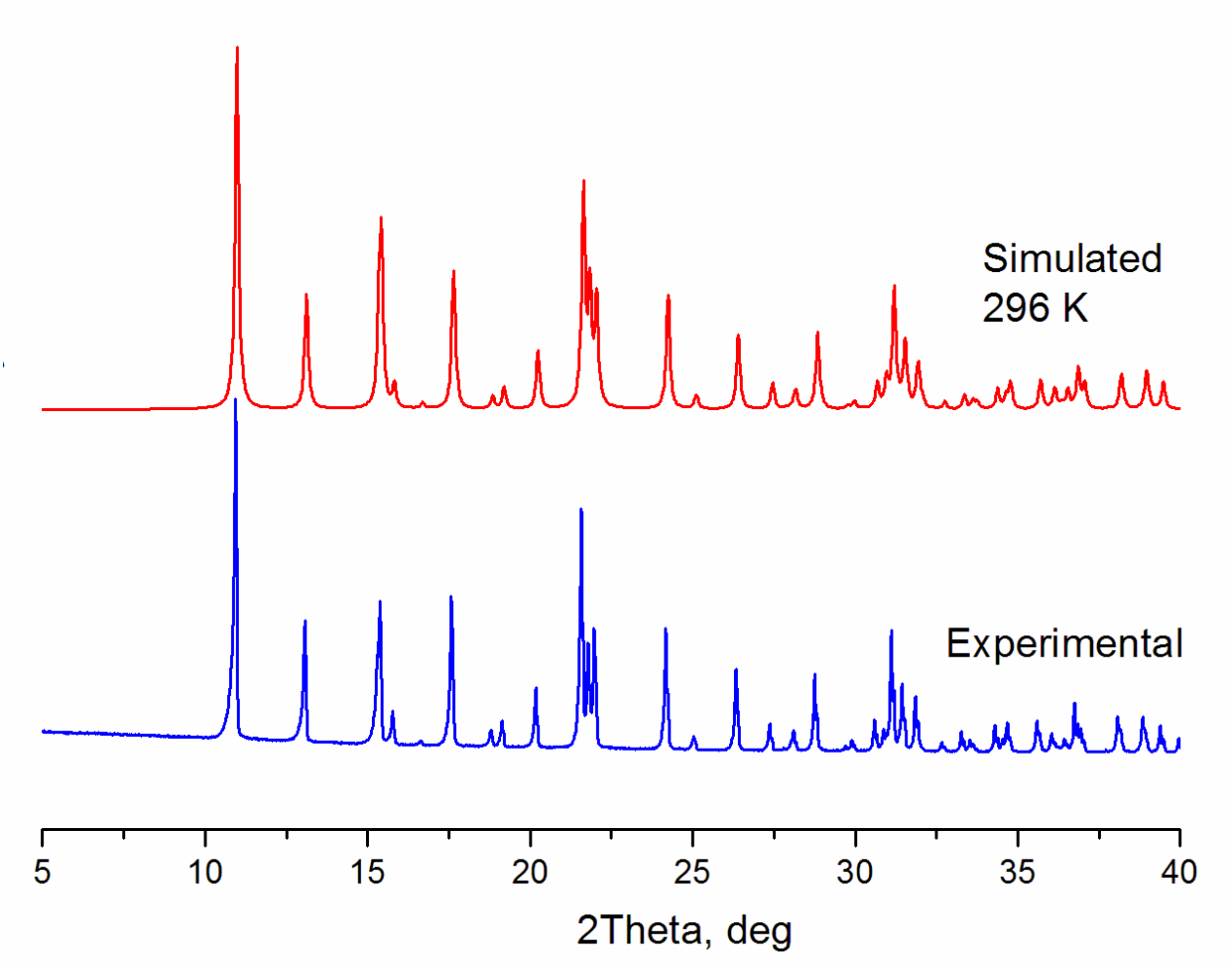

Figure S4. Simulated (top) and experimental (bottom) powder XRD patterns of *trans*-[Pt(thm)$_2$Cl$_2$] (complex **5**) (CuKα radiation). The simulated pattern was calculated using PLATON program.

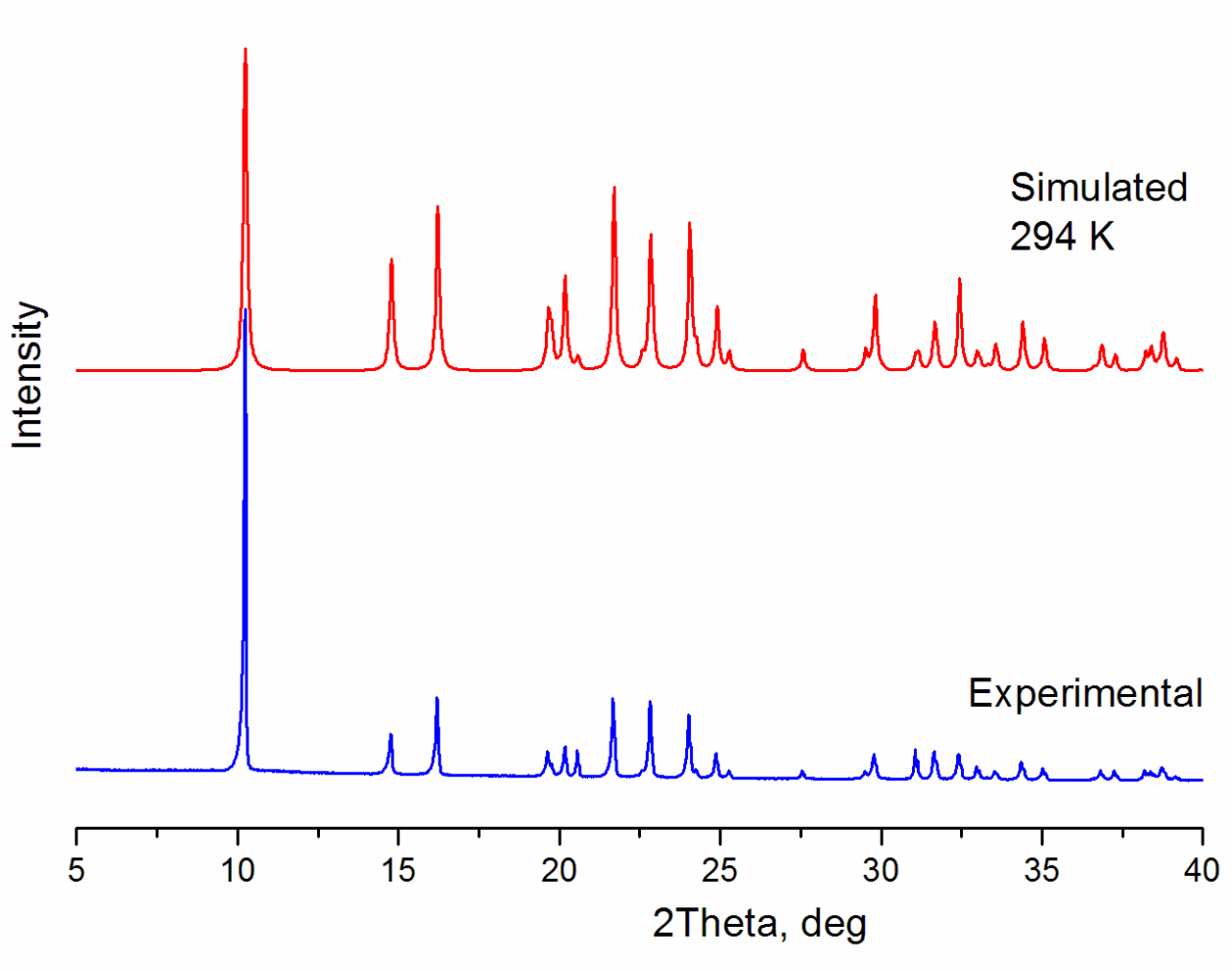

Figure S5. Simulated (top) and experimental (bottom) powder XRD patterns of *trans*-[Pd(het)$_2$Cl$_2$] (complex **6**) (CuKα radiation). The simulated pattern was calculated using PLATON program.

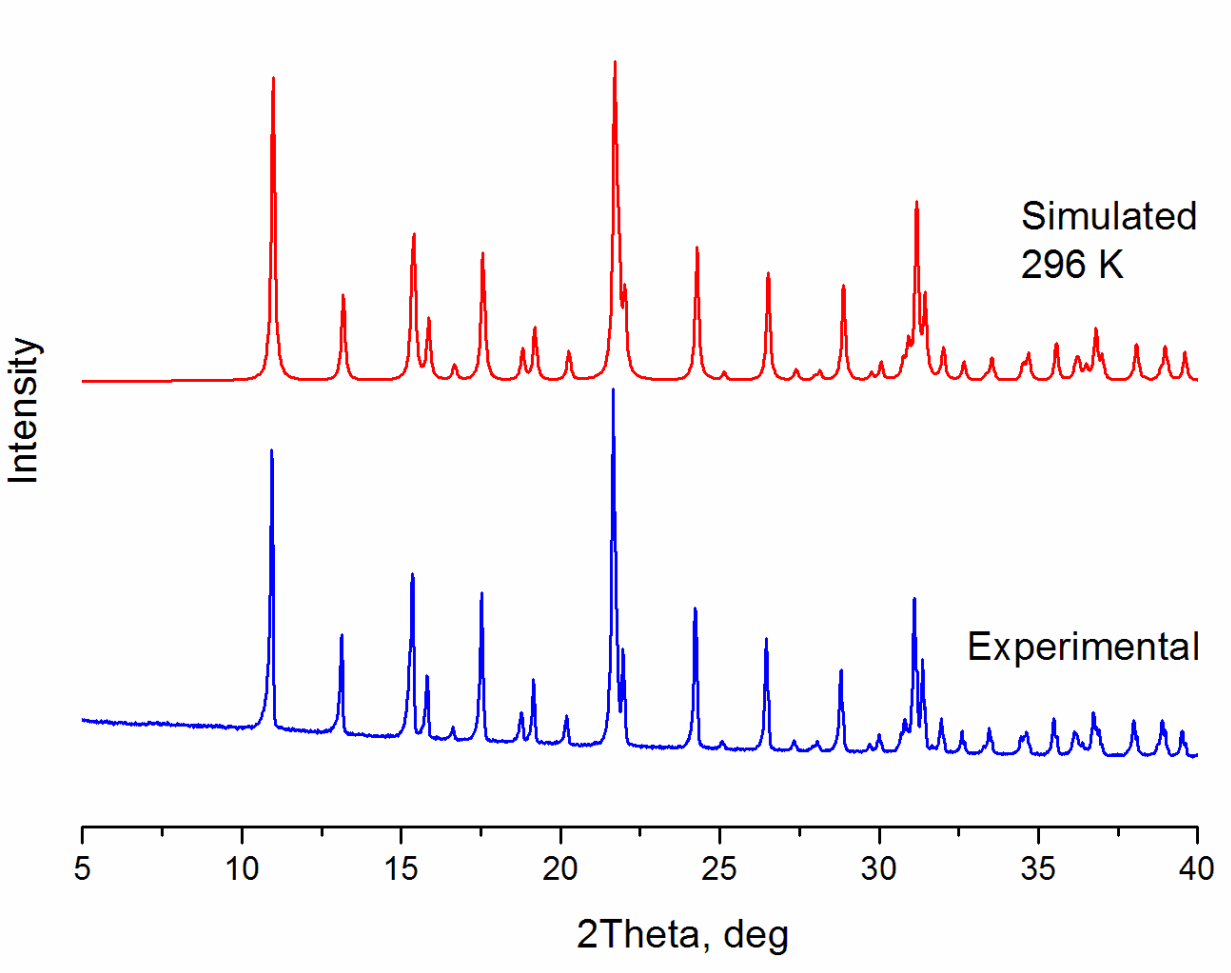

Figure S6. Simulated (top) and experimental (bottom) powder XRD patterns of *trans*-$[Pd(thm)_2Cl_2]$ (complex **7**) (CuKα radiation). The simulated pattern was calculated using PLATON program.

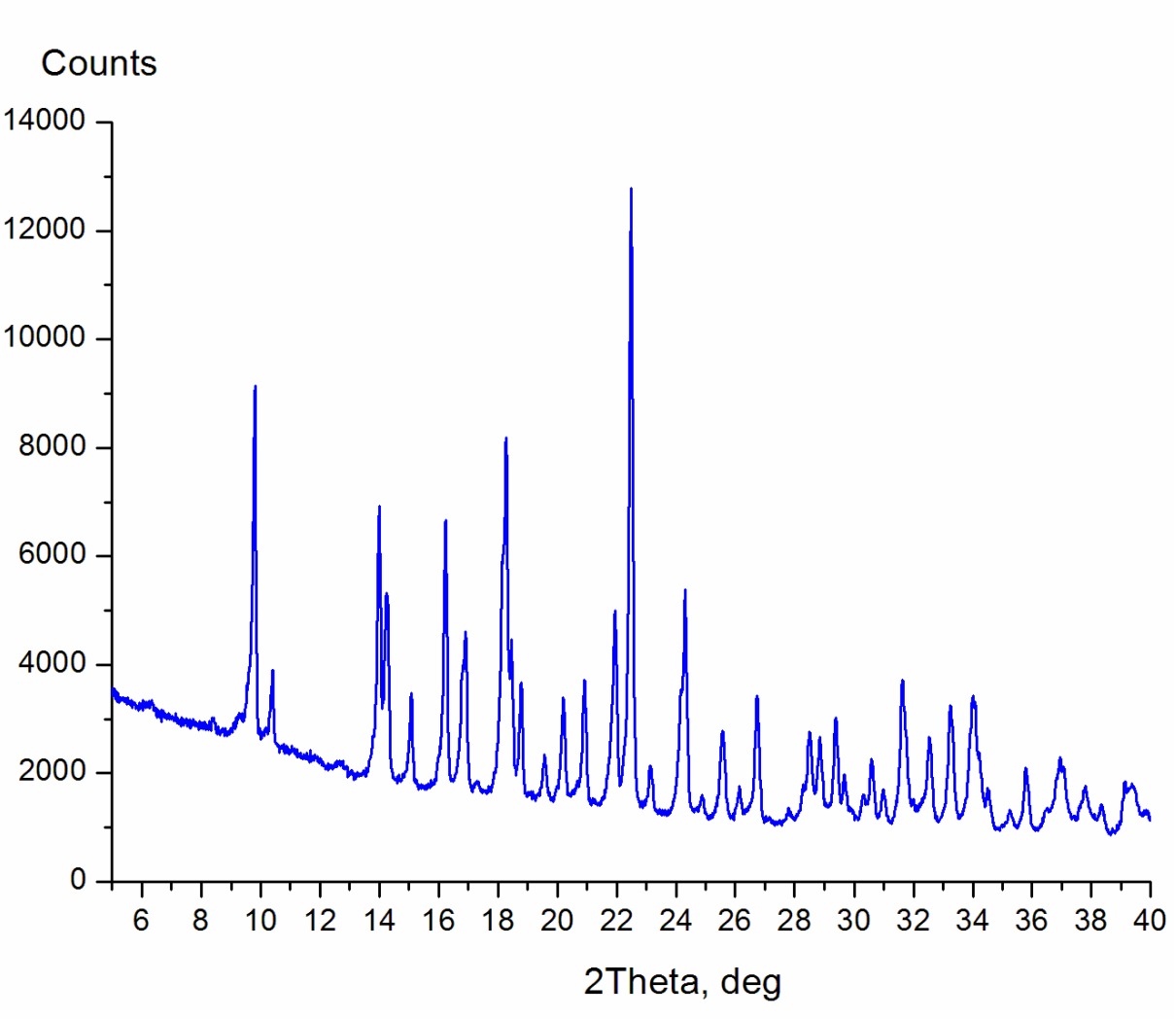

Figure S7. Experimental powder XRD of *cis*-[Pt(het)$_2$Cl$_2$] (complex **3**) (CuKα radiation).